Clinical Cancer Research

Therapeutic Inhibition of the MDM2–p53 Interaction Prevents Recurrence of Adenoid Cystic Carcinomas

Felipe Nör[1,2], Kristy A. Warner[1], Zhaocheng Zhang[1], Gerson A. Acasigua[1,2], Alexander T. Pearson[1,3], Samuel A. Kerk[1], Joseph I. Helman[4,5], Manoel Sant'Ana Filho[2], Shaomeng Wang[3,5,6,7], and Jacques E. Nör[1,5,8,9]

Abstract

Purpose: Conventional chemotherapy has modest efficacy in advanced adenoid cystic carcinomas (ACC). Tumor recurrence is a major challenge in the management of ACC patients. Here, we evaluated the antitumor effect of a novel small-molecule inhibitor of the MDM2–p53 interaction (MI-773) combined with cisplatin in patient-derived xenograft (PDX) ACC tumors.

Experimental Design: Therapeutic strategies with MI-773 and/or cisplatin were evaluated in SCID mice harboring PDX ACC tumors (UM-PDX-HACC-5) and in low passage primary human ACC cells (UM-HACC-2A, -2B, -5, -6) *in vitro*. The effect of therapy on the fraction of cancer stem cells (CSC) was determined by flow cytometry for ALDH activity and CD44 expression.

Results: Combined therapy with MI-773 with cisplatin caused p53 activation, induction of apoptosis, and regression of ACC PDX tumors. Western blots revealed induction of MDM2, p53 and downstream p21 expression, and regulation of apoptosis-related proteins PUMA, BAX, Bcl-2, Bcl-x_L, and active caspase-9 upon MI-773 treatment. Both single-agent MI-773 and MI-773 combined with cisplatin decreased the fraction of CSCs in PDX ACC tumors. Notably, neoadjuvant MI-773 and surgery eliminated tumor recurrences during a postsurgical follow-up of more than 300 days. In contrast, 62.5% of mice that received vehicle control presented with palpable tumor recurrences within this time period ($P = 0.0097$).

Conclusions: Collectively, these data demonstrate that therapeutic inhibition of MDM2–p53 interaction by MI-773 decreased the CSC fraction, sensitized ACC xenograft tumors to cisplatin, and eliminated tumor recurrence. These results suggest that patients with ACC might benefit from the therapeutic inhibition of the MDM2–p53 interaction. *Clin Cancer Res; 23(4); 1036–48. ©2016 AACR.*

Introduction

Salivary gland tumors are typically not responsive to conventional chemotherapy. Adenoid cystic carcinoma (ACC) is one of the most common malignancies arising from minor and major salivary glands (1). Despite the apparent "benign" behavior characterized by slow tumor growth, ACC is relentless. It is highly destructive to adjacent anatomic sites and exhibits a high frequency of perineural invasion events that leads to severe morbidity, particularly as this tumor grows toward the brain (2). The slow and indolent clinical course often leads to a late diagnosis, when tumor is already at advanced stages and systemic intervention is required to prevent distant metastasis and recurrence after surgical resection. Unfortunately, current standard chemotherapy (e.g., platinum-based drugs) has shown limited long-term efficacy in ACC patients (3–5). The prevalence of recurrence is high mainly due to late hematogenous dissemination of cancer cells primarily to lungs, bone, and liver (4). Novel mechanism-based therapies to overcome drug resistance are desperately needed to enhance the survival and quality of life for patients with ACC.

The mechanisms involved in the resistance of ACC to chemotherapy are poorly understood. The first-line chemotherapy for ACC often includes cisplatin, which is frequently combined with other classes of antineoplastic agents [e.g., 5-fluorouracil (5-FU); refs. 3, 6]. However, data from clinical trials with these drug combinations are not promising, with modest efficacy in ACC (7). The combination of cisplatin with doxorubicin and cyclophosphamide mediated only partial therapeutic responses (8). Another study tested the efficacy of combination cisplatin, 5-FU, and epirubicin in patients with advanced, symptomatic ACC (9). From 8 patients enrolled in this study, one showed partial response to therapy and 5 had stable disease. Besides the low sample size, one important limitation of this study is the total

[1]Department of Cariology, Restorative Sciences, and Endodontics, University of Michigan School of Dentistry, Ann Arbor, Michigan. [2]Department of Oral Pathology, Universidade Federal do Rio Grande do Sul, Porto Alegre, Rio Grande do Sul, Brazil. [3]Department of Internal Medicine, University of Michigan School of Medicine, Ann Arbor, Michigan. [4]Department of Oral and Maxillofacial Surgery, University of Michigan School of Dentistry, Ann Arbor, Michigan. [5]University of Michigan Comprehensive Cancer Center, Ann Arbor, Michigan, USA. [6]Department of Pharmacology, University of Michigan School of Medicine, Ann Arbor, Michigan. [7]Department of Medicinal Chemistry, University of Michigan College of Pharmacy, Ann Arbor, Michigan. [8]Department of Otolaryngology, University of Michigan School of Medicine, Ann Arbor, Michigan. [9]Department of Biomedical Engineering, University of Michigan College of Engineering, Ann Arbor, Michigan.

Note: Supplementary data for this article are available at Clinical Cancer Research Online (http://clincancerres.aacrjournals.org/).

Corresponding Author: Jacques E. Nör, University of Michigan, 1011 N. University Rm. 2353, Ann Arbor, MI 48109-1078. Phone: 734-936-9300; Fax: 734-936-9300; E-mail: jenor@umich.edu

doi: 10.1158/1078-0432.CCR-16-1235

AACR

Translational Relevance

Adenoid cystic carcinoma (ACC) is a relentless form of salivary gland cancer, typically treated with surgery and radiation, as these tumors are resistant to chemotherapy. In advanced disease, cisplatin is usually the first treatment option, but clinical response and long-term efficacy are modest at best. Here, we demonstrate that therapeutic inhibition of the MDM2–p53 interaction with a small molecule (MI-773) sensitizes adenoid cystic carcinomas to cisplatin in patient-derived xenograft (PDX) and low passage primary human ACC models. Combination of MI-773 and cisplatin mediates potent and durable tumor regression via p53 reactivation and tumor cell apoptosis. MI-773 reduces the fraction of cancer stem cells, which have been associated with resistance to therapy. Notably, neoadjuvant therapy with MI-773 and cisplatin eliminated recurrences of PDX ACC tumors for at least 300 days. Collectively, these data suggest that patients with ACC might benefit from combination therapy with a MDM2–p53 inhibitor and cisplatin.

period of evaluation (62.3 months), when it is known that around half of ACCs recur only after 10 years (10). Notably, most ACC tumors express the proto-oncogene c-KIT. However, dasatinib (a c-KIT inhibitor) was not effective in a phase II clinical trial with ACC patients (11). The scarcity of preclinical/clinical evidence and lack of response to conventional drugs in the daily clinical practice is reflected on the most recent guideline from the National Comprehensive Cancer Network (NCCN), in which no specific chemotherapeutic drug/regimen is indicated for the treatment of these patients. To improve the prediction of patient outcomes, NCCN has incorporated nomograms (i.e., statistical model using regression analysis) to guidelines as an alternative method for TNM staging system. Notably, this method was proven to be accurate in the prediction of survival and recurrence in ACC patients (12).

The tumor suppressor p53 is often inactivated in cancer (13). Important functions of wild-type p53 (e.g., cell-cycle control, DNA repair, induction of apoptosis) are regulated by its interaction with murine double minute 2 (MDM2; ref. 14). This protein interaction forms an autoregulatory negative feedback loop, that is, nuclear p53 induces the expression of MDM2, which in turn binds directly to p53, provoking its degradation through the 26S proteasomal pathway. This interaction is important to maintain low cellular levels of p53 in physiologic conditions (14, 15). However, overexpression of MDM2 leads to p53 inactivation, which contributes to tumorigenic processes (16). Of note, MDM2 expression levels have been associated with tumor progression and poor prognosis of ACC patients (17, 18).

Recently, Wang and colleagues have developed a small-molecule inhibitor of the MDM2–p53 interaction (MI-773, patented by Sanofi as SAR405838), pursuing the p53 activation as a new anticancer strategy (19). MI-773 has a high binding affinity to MDM2 ($K_i = 0.88$ nmol/L), preventing MDM2 interaction with p53. Indeed, MI-773 is capable of wild-type p53 reactivation in cancer cell lines and several preclinical models of cancer, for example, osteosarcoma, leukemia, colon, and prostate cancer (19, 20). Considering the important role of MDM2 in ACC, our group has tested the effect of MI-773 in preclinical models of ACC

(21). We observed that therapeutic inhibition of MDM2 with MI-773 restored p53 function, as shown by the activation of its downstream-related protein (i.e., p21). Here, we went a step further and evaluated the effect of MI-773 in combination with cisplatin in preclinical models of ACC. MI-773 and cisplatin drug combination induced robust and durable ACC tumor regression. Furthermore, this therapy significantly decreased the proportion of cancer stem cells (CSC), which has been associated with cisplatin resistance in head and neck tumors (22). Collectively, these results suggest that patients with ACC might benefit from neoadjuvant therapeutic inhibition of the MDM2–p53 interaction combined with conventional chemotherapy with cisplatin.

Materials and Methods

Salivary ACC cells

Primary cell cultures were generated from human tumor specimens and named "University of Michigan Human Adenoid Cystic Carcinoma (UM-HACC)" series, as described previously (21, 23). UM-HACC-2A, UM-HACC-2B, UM-HACC-5, and UM-HACC-6 cells were maintained in salivary gland culture media, that is, high-glucose DMEM (Invitrogen) supplemented with 2 mmol/L L-glutamine (Invitrogen), 1% antibiotic (AAA; Sigma-Aldrich), 10% FBS (Invitrogen), 20 ng/mL EGF (Sigma-Aldrich), 400 ng/mL hydrocortisone (Sigma-Aldrich), 5 µg/mL insulin (Sigma-Aldrich), 50 ng/mL nystatin (Sigma-Aldrich), and 1% amphotericin B (Sigma-Aldrich). Cells were passed using 0.05% trypsin/EDTA (Invitrogen) and used for up to 20 passages. Therefore, these cells are considered here low-passage primary ACC cells (instead of established cell lines). UM-HACC-2A is a low passage cell culture derived from an aggressive primary tumor, and UM-HACC-2B represents ACC cells derived from the lymph node metastasis of the same patient. UM-HACC-5 cells were obtained from a patient that had histologic confirmation of perineural and bone invasion, and UM-HACC-6 cells were derived from a recurrent tumor diagnosed 15 years after initial diagnosis and also presented perineural invasion. All low passage ACC cell cultures used here express wild-type p53 (21).

Studies with patient-derived xenograft model of ACC

Patient-derived xenograft (PDX) models have been increasingly used in translational cancer research (24). Tumor fragments from a PDX model of ACC (UM-PDX-HACC-5; refs. 21, 23) at in vivo passages 5 to 6 were transplanted into the subcutaneous space of the dorsum of SCID mice (CB.17.SCID; Charles River Laboratories). Tumor volume was calculated using the formula: volume (mm³) = $L \times W^2/2$ (L, length; W, width). All tumors were surgically retrieved when they reached our UCUCA-approved cutoff volume of 2,000 mm³. The protocol for animal care was reviewed and approved by appropriate University of Michigan institutional committees. Mice transplanted with UM-PDX-HACC-5 tumors were randomly allocated into four groups ($n = 5$–6), maintaining the average of tumor volume (500 mm³/group). Experimental conditions were as follows: vehicle control (saline, intraperitoneally, weekly); 5 mg/kg cisplatin (intraperitoneally, weekly); 200 mg/kg MI-773 (gavage, weekly); or the combination of 5 mg/kg cisplatin + 200 mg/kg MI-773 regimens. Treatment was administered for 30 days, mice were followed for additional 24 days, and then mice were euthanized and tumors retrieved. To compare weekly versus daily regimens of MI-773 combined with fixed doses of cisplatin, 200 mg/kg

MI-773 was divided into equable daily doses (i.e., 28.5 mg/kg MI-773). When tumor reached an average volume of 200 mm^3, animals were randomly distributed into the experimental groups ($n = 7$–8). Treatment was administered for 14 days, and mice were followed for additional 44 days, when experiment was terminated and tumors were collected. To evaluate tumor recurrence, animals were submitted to a neoadjuvant regimen of MI-773. Briefly, mice transplanted with UM-PDX-HACC-5 tumors (average volume of 500 mm^3) were divided into two groups ($n = 8$): vehicle control (polyethylene gycol-200 + D-α-tocopherol polyethylene glycol 1000 succinate; Sigma-Aldrich) or 200 mg/kg MI-773. Initially, animals received either a single dose of MI-773 or vehicle. After 7 days, tumors were surgically removed and incisions were closed with Vetbond (3M). Weekly treatments restarted 7 days after surgery and continued for 30 days. Then, mice were examined twice per week for 300 days for signs of recurrence, as defined as the presence of palpable tumor.

Flow cytometry

Salivary gland CSCs were identified as ALDH^{high}CD44^{high} cells, as described previously (25, 26). UM-PDX-HACC-5 tumors were collected, cut in small pieces, and dissociated using the gentle-MACS Dissociator Kit (Miltenyi Biotec), incubated in ACK red blood cell lysis buffer (Invitrogen), and filtered through a 40-μm sterile cell strainer. Cells were incubated with 5 μL activated Aldefluor substrate (BAA) or 5 μL aldehyde dehydrogenase (ALDH) inhibitor (DEAB), using the Aldefluor Kit (Stem Cell Technologies) for 40 minutes at 37°C. A monoclonal mouse anti-human CD44 antibody (1:60; APC-cat #559942, PE-cat #550989; BD Pharmingen) was incubated for 30 minutes at 4°C, and human cells were separated from murine cells using anti-HLA-ABC (PE-cat #560168; BD Pharmingen). Viable cells were stained using 7-AAD (cat #00-6993-50; eBioscience). For cell-cycle analysis, $5 × 10^5$ UM-HACC-5 or UM-HACC-6 cells were treated with either vehicle control, MI-773, and/or cisplatin diluted in salivary gland medium for 24 hours. After harvesting, cells were fixed in 70% cold ethanol and exposed to 0.1% sodium citrate, 25 μg/mL propidium iodide (Sigma-Aldrich), 100 μg/mL RNase A, and 0.1% Triton X-100. Flow cytometry (FACSCalibur; BD Biosciences) was carried out to quantify the percentage of cells in each cell-cycle phase (G$_0$–G$_1$, S, and G$_2$–M), as described previously (23). Data were obtained from triplicates and represent at least three independent experiments. Results were analyzed using FlowJo software (FlowJo, LLC).

Subcellular fractionation

Cytoplasmic and cellular membrane portions were separated from the nucleus, as described previously (27). Briefly, UM-HACC-5 cells were treated with vehicle control, Cisplatin and/or MI-773 for 24 hours. Then, cells were resuspended in cytoplasmic extraction buffer (Panomics) and incubated for 3 minutes on ice. The suspension was centrifuged at 13,000 rpm for 5 minutes at 4°C. Supernatant was collected as cytoplasmic/cell membrane extract. The remaining pellet was resuspended in nuclear extraction buffer (Panomics) with occasional vortexing during 40 minutes. After centrifugation, the supernatant was collected as nuclear extract.

Western blots

Protein lysates from UM-PDX-HACC-5 tumors, UM-HACC-5, and UM-HACC-6 cells were prepared using 1% Nonidet P-40 (NP-40) lysis buffer and loaded onto 9% to 12% SDS-PAGE gels. Membranes were incubated with the following primary antibodies overnight at 4°C: mouse anti-human p53 (1:1,000), β-actin conjugated with horseradish peroxidase (HRP; 1:100,000), rabbit anti-hnRNP (1:1,000) (Santa Cruz Biotechnology); hamster anti-human Bcl-2 (1:500), rabbit anti-human phospho-p53 (S392; 1:1,000), p21 (1:2,000), BAX (1:500), PUMA (1:500), cleaved-caspase 9 (1:1,000) (Cell Signaling Technology); mouse anti-human MDM2 (1:500; Thermo Fisher Scientific); rabbit anti-human Bcl-x$_L$ (1:500; BD Biosciences), or mouse anti-GAPDH (1:1,000,000; Chemicon). Membranes were exposed to affinity-purified secondary antibodies (1:1,000) conjugated with HRP (The Jackson Laboratory), and immunoreactive proteins were visualized by SuperSignal West Pico chemiluminescent substrate (Thermo Scientific).

Cytotoxicity assays

Sulforhodamine B (SRB) assays were performed to evaluate the effect of treatment on ACC cell viability, as described previously (23). Here, $2 × 10^3$ UM-HACC-5 and UM-HACC-6 cells per well were exposed to vehicle, MI-773, and/or cisplatin for 24 to 96 hours. After fixation with 10% cold trichloroacetic acid for 1 hour at 4°C, viable cells were stained by addition of 0.4% SRB dye (Sigma-Aldrich) for 30 minutes at room temperature. The excess unbound dye was removed by 1% acetic acid. SRB-stained cells were resolubilized in 10 mmol/L unbuffered Tris base, and plates were read in a microplate reader at 560 nm (GENios, Tecan). Results were normalized by vehicle control and IC$_{50}$ values were determined. Data were obtained from quadruplicate wells/condition and represent at least three independent experiments.

Fluorometric assay

UM-HACC-5, -6 cells were treated with IC$_{50}$ concentrations of MI-773, cisplatin, or vehicle control for 24 hours. Cell pellets were resuspended in lysis buffer, and cells were incubated with 1 mmol/L IETD-AFC (caspase-8 substrate; Enzo) or 1 mmol/L LEHD-AFC (caspase-9 substrate; Enzo) for up to 2 hours at 37°C. Samples were analyzed in a microplate reader at 400 nm (GENios).

Statistical analyses

Data were analyzed by one-way ANOVA, followed by *post hoc* tests (Tukey) for multiple comparisons or Student *t* test, when indicated. Regression modeling was performed using mixed effect linear regression to account for repeated measures on each tumor. The tumor volume data was log transformed to account for exponential growth. Model fixed effects included time, cisplatin treatment, and MI-773 treatment, and tumor starting size. Random effects included mouse. We assumed an autoregressive correlation structure where more proximate time values have a higher degree of correlation. When comparing different dosing schemas, each dosing category was included as a different factor level in the regression model. Predictions curves were generated directly from the regression model. Kaplan–Meier graphs were analyzed by the Gehan–Breslow–Wilcoxon test. Failure criterion was a 2-fold increase in tumor volume (for tumor growth analysis) or presence of palpable tumor (for recurrence analysis). Significance level (α) was determined at $P < 0.05$. Analysis was performed using the "survival" and "gls" packages in software program, version R 3.1.0.

Results

MI-773 sensitizes ACC PDX tumors to cisplatin

To begin to understand the effect of combining MI-773 with cisplatin *in vivo*, we performed a pilot study to evaluate drug toxicity. Using published studies as reference, we choose weekly doses of 5 mg/kg cisplatin (22) and 200 mg/kg MI-773 (21) for this experiment. Weight loss did not exceed 20% (compared with pretreatment values), which is our UCUCA-approved cutoff for systemic toxicities, when we used single-agent cisplatin or MI-773 or combination of both drugs (Supplementary Fig. S1). To evaluate the effect of MI-773 and/or cisplatin on UM-HACC-PDX-5 tumors, we allowed tumors to grow to an average volume of 500 mm^3 and then began treating mice with the same doses mentioned above for 30 days (Fig. 1). We observed that MI-773 as a single agent causes tumor regression, being more effective than single-agent cisplatin (Fig. 1A and C). Cisplatin therapy shows limited therapeutic response, stabilizing the tumor growth, but not causing PDX tumor regression, as reported in humans (6–9). However, combination of MI-773 and cisplatin was more effec-

tive than single-agent therapy. There was no tumor rebound upon termination of treatment within the duration of the follow-up in this initial experiment (about 20 days posttreatment; Fig. 1A). Importantly, mice did not show weight loss beyond the 20% cutoff (Fig. 1B). We performed linear mixed effect regression modeling on the tumor volume to account for repeated measures on each tumor and determine the effects of time, cisplatin treatment, MI-773 treatment, and starting tumor size on tumor volume. The rate of tumor growth was significantly less in MI-773 ($P = 0.0002$) and cisplatin ($P = 0.0017$) groups when compared with control (Fig. 1C). Western blot analysis from UM-HACC-PDX-5 tumors shows that therapeutic inhibition of MDM2, combined or not with cisplatin, causes the upregulation of p53 and MDM2 expression (Fig. 1D). MI-773–activated p53 is functional *in vivo*, as confirmed by the upregulation of its downstream protein p21 and the apoptosis effector protein BAX. In contrast, PUMA appears to be primarily regulated by cisplatin, while the prosurvival protein Bcl-2 did not show considerable changes in expression levels upon treatment. Collectively, these *in vivo* results
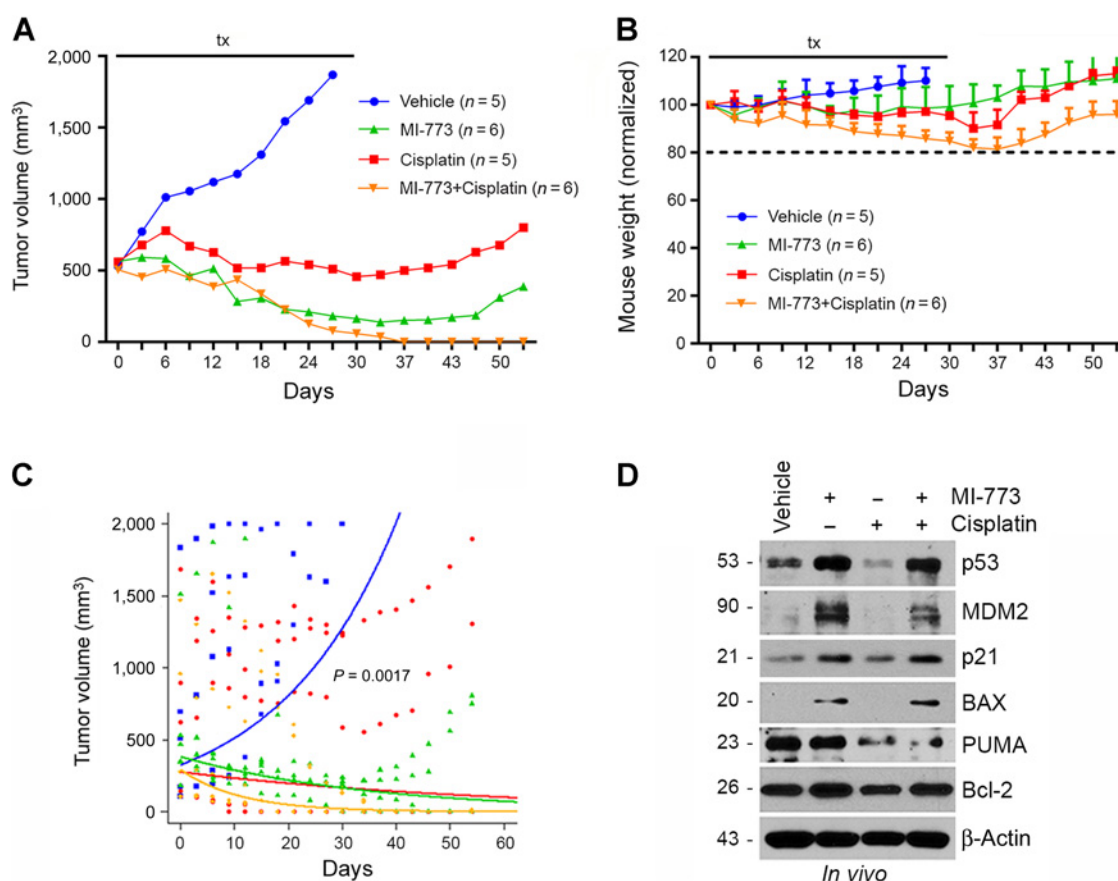

Figure 1.
Effect of MI-773 and/or cisplatin in a preclinical model of ACC. UM-PDX-HACC-5 tumors were transplanted in immunodeficient mice. When tumors reached 500 mm^3, animals were randomly allocated into four different treatment regimens as follows: 5 mg/kg saline (vehicle control), 200 mg/kg MI-773, 5 mg/kg cisplatin, or 200 mg/kg MI-773 combined with 5 mg/kg cisplatin weekly. **A,** Graph depicting tumor volume during treatment (tx) and follow-up (23 days) periods. Cisplatin stabilized tumor growth, while MI-773 decreases tumor volume compared with pretreatment values. MI-773 combined with cisplatin ablates tumor in the majority of animals and prevents tumor regrowth after treatment. **B,** Graph depicting mouse weight during the experimental period. Data were normalized against pretreatment weight. **C,** Graph depicting a linear regression model using repeated measures for each tumor over time. MI-773 and/or cisplatin significantly decrease the tumor growth rate when compared with vehicle control. **D,** Western blot analysis for p53, MDM2, p21, BAX, PUMA, and Bcl-2 in UM-PDX-HACC-5 tumors treated with either MI-773 and/or cisplatin as compared with vehicle control. Tumors were harvested 23 days after the last administration of drugs.

demonstrate that MI-773 mediates ACC tumor regression in a preclinical model of ACC.

Effect of MI-773 and/or cisplatin on ACC cell proliferation and survival

To evaluate the therapeutic potential of each drug *in vitro*, low passage primary human ACC cells (UM-HACC-5 and UM-HACC-6) were treated with either a dose range of MI-773 (0.01–10 μmol/L) or cisplatin (0.02–20 μmol/L). Alternatively, cells were treated with a fixed dose of cisplatin (2 μmol/L) together with increasing concentrations of MI-773. The percentage of viable cells was determined by SRB assay. Data were normalized against vehicle control. We observed a dose- and time-dependent cytotoxic response in both ACC primary cells evaluated. IC_{50} values for single agent were in the low micromolar range, and for both ACC cells, the IC_{50} for MI-773 was about half concentration as compared with the IC_{50} for cisplatin (Fig. 2A). Combination of both agents further reduced the IC_{50} to 0.73 μmol/L (UM-HACC-5) and 3.79 μmol/L (UM-HACC-6) at 72 hours (Fig. 2A). Representative photomicrographs of cells in culture conditions were taken after 72 hours of treatment using intermediate doses of single or combined drugs regimens (1–2 μmol/L; Supplementary Fig. S2B). To better understand the mechanisms associated with the antitumor effect observed *in vivo*, UM-PDX-HACC-5 tissue slides were stained for *in situ* TUNEL to reveal cells undergoing apoptosis (Fig. 2B). The percentage of TUNEL-positive cells is significantly higher ($P < 0.05$) in animals that received either MI-773 or cisplatin (Fig. 2B and C). Combination therapy induced more apoptosis than cisplatin or MI-773 used as a single agent (Fig. 2C). In addition, we evaluated the effect of treatment on cell cycle. UM-HACC-5 or UM-HACC-6 cells were treated for 24 hours using low concentrations of either MI-773 and/or cisplatin (1–2 μmol/L), and the percentage of cells in each cell-cycle phase was determined by flow cytometry (Supplementary Fig. S3). MI-773 causes cell-cycle arrest at the first checkpoint (G_1); a similar trend is seen upon drug combination therapy. As previously reported (28), the majority of cells exposed to cisplatin are retained in the S-phase (Fig. 2D). Taken together, these results indicate that antitumor cell effects seen upon treatment with MI-773 and/or cisplatin involve cell-cycle arrest and induction of apoptosis.

Inhibition of the MDM2–p53 interaction with MI-773 activates p53

To better understand the role of MI-773 on p53 activation in ACC, we first performed Western blot analysis for the basal expression of MDM2 and apoptosis-related proteins (i.e., Bcl-x_L and Bcl-2) in UM-HACC-2A, UM-HACC-2B, UM-HACC-5, and UM-HACC-6 cells (Fig. 3A). Next, we treated ACC cells with single-agent MI-773 or cisplatin at intermediate doses (1–2 μmol/L) and observed that p53, MDM2, p21, BAX, and PUMA (except for UM-HACC-6 cells) expression is increased with MI-773, while Bcl-2 expression was slightly decreased upon treatment with cisplatin (Fig. 3B). Then, we evaluated more closely the expression of p53 in UM-HACC-PDX-5 tumors from experiment reported in Fig. 1. Tumors treated with either vehicle or cisplatin show nuclear localization of p53. Surprisingly, the administration of MI-773 as a single agent or combined with cisplatin causes a partial translocation of p53 to the cytoplasm (Fig. 3C). To confirm this apparent translocation of p53, we exposed UM-HACC-5 cells to low concentrations of MI-773 and/or cisplatin (0.1–0.2 μmol/L). After 24 hours, we performed a subcellular fractionation
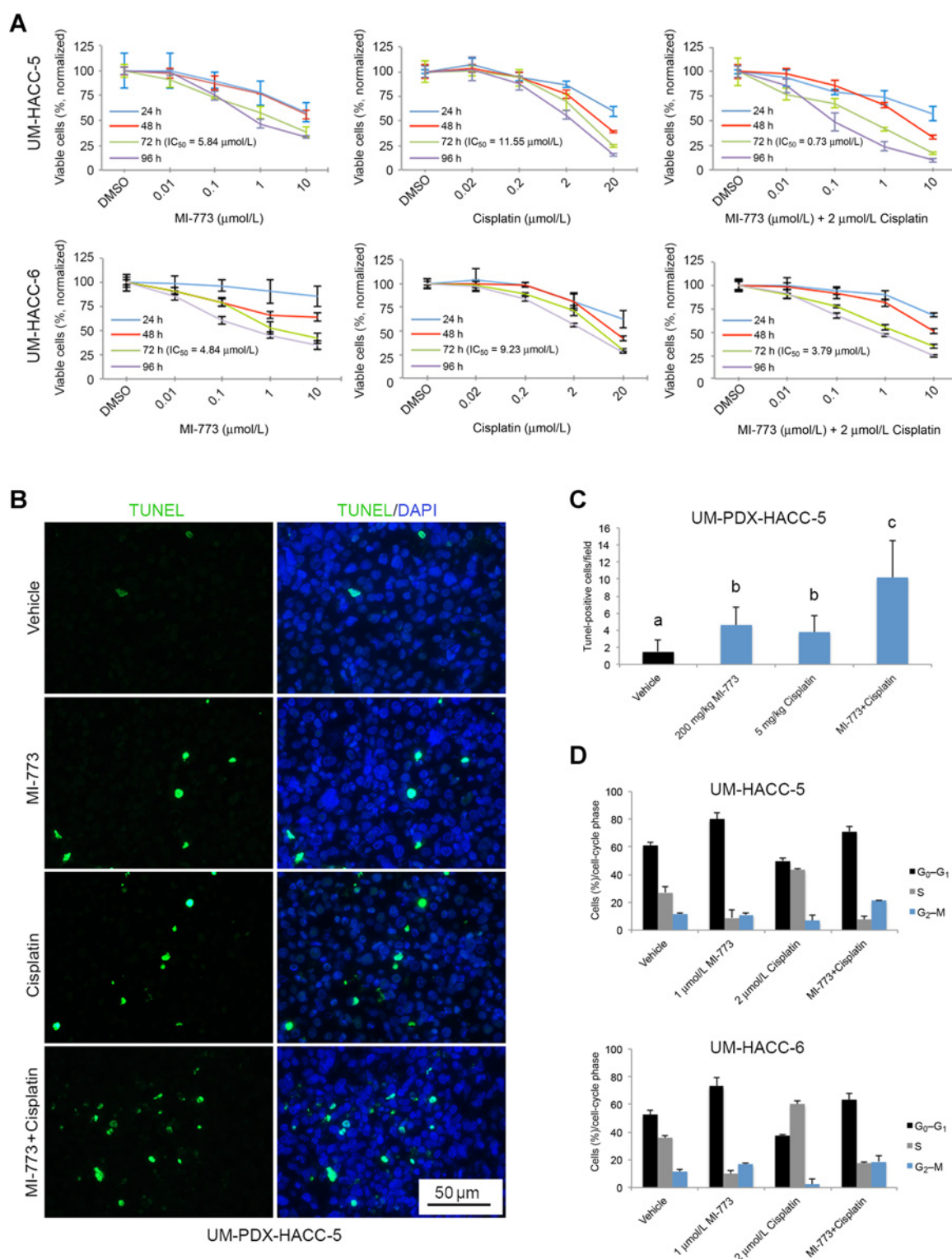
assay to separate the nucleus compartment from the cytoplasm/membrane components. Confirming the data obtained by IHC, tumors exposed to MI-773 alone or in combination with cisplatin presented p53 in both nucleus and cytoplasm. MI-773 caused a robust increase in MDM2 expression, which was observed in both the nuclear and the cytoplasmic extract (Fig. 3D). Immunofluorescence further confirmed the cytoplasmic presence of p53 upon treatment with MI-773 (Fig. 3E).

To further understand the effect of MI-773 or cisplatin on ACC cells, we performed a series of dose- and time-dependent experiments (Fig. 4). MI-773 induces activation of phospho-p53 (SER 392), p53, MDM2, p21, BAX, and PUMA in a dose-dependent manner, with visible effects already being observed with 0.1 μmol/L in both cell lines (Fig. 4A). The prosurvival protein Bcl-x_L appears to be upregulated by low concentration MI-773 in both ACC cells and went down to baseline levels at 10 μmol/L (Fig. 4A). Cisplatin requires higher doses for the activation of p53, MDM2, p21, and BAX when compared with MI-773 (Fig. 4A and B). The activation of BAX by cisplatin appears to be associated with Bcl-x_L downregulation and does not involve PUMA regulation, which differs from MI-773 treatment.

In a time course evaluation with intermediate dose of MI-773 (1 μmol/L), p53 and p21 were constantly activated over 96 hours, while the expression of MDM2 increased with time particularly in UM-HACC-6 cells (Fig. 4C). Upon cisplatin treatment (2 μmol/L), the peak of p53 activation was at 48 hours in UM-HACC-5 cells; the same trend was observed for MDM2. In UM-HACC-6 cells, p53 activation was constant, but MDM2 expression increased over time (Fig. 4D). To better understand the effect of drugs together, we designed an experiment to evaluate the effect of minimal doses of MI-773 and cisplatin on p53 and MDM2. We observed that MI-773 appears to be the dominant factor driving p53 and MDM2 expression when used in combination with cisplatin in the four low passage ACC cell cultures tested here (Fig. 4E). Collectively, these results demonstrate that MI-773 induces p53, MDM2, and p21 expression via a mechanism that is associated with upregulation of Bax and PUMA. To further understand the mechanisms involved in MI-773–induced apoptosis, we performed fluorometric assays. They revealed that caspase-9 (but not caspase-8) is activated upon treatment of ACC cells with MI-773 and/or cisplatin (Fig. 4G). Of note, the activation of caspase-9 in UM-HACC-5 cells treated with MI-773 + cisplatin (120 minutes) is 5.94-fold higher than vehicle control, and in UM-HACC-6, it is 6.76-fold higher than vehicle (Fig. 4G). These data indicate that this drug combination is equally effective in both ACC cell cultures. Western blots were used to verify the data obtained with the fluorometric assay and confirmed that treatment with MI-773 and/or cisplatin induces expression of cleaved (active) caspase-9 (Fig. 4F).
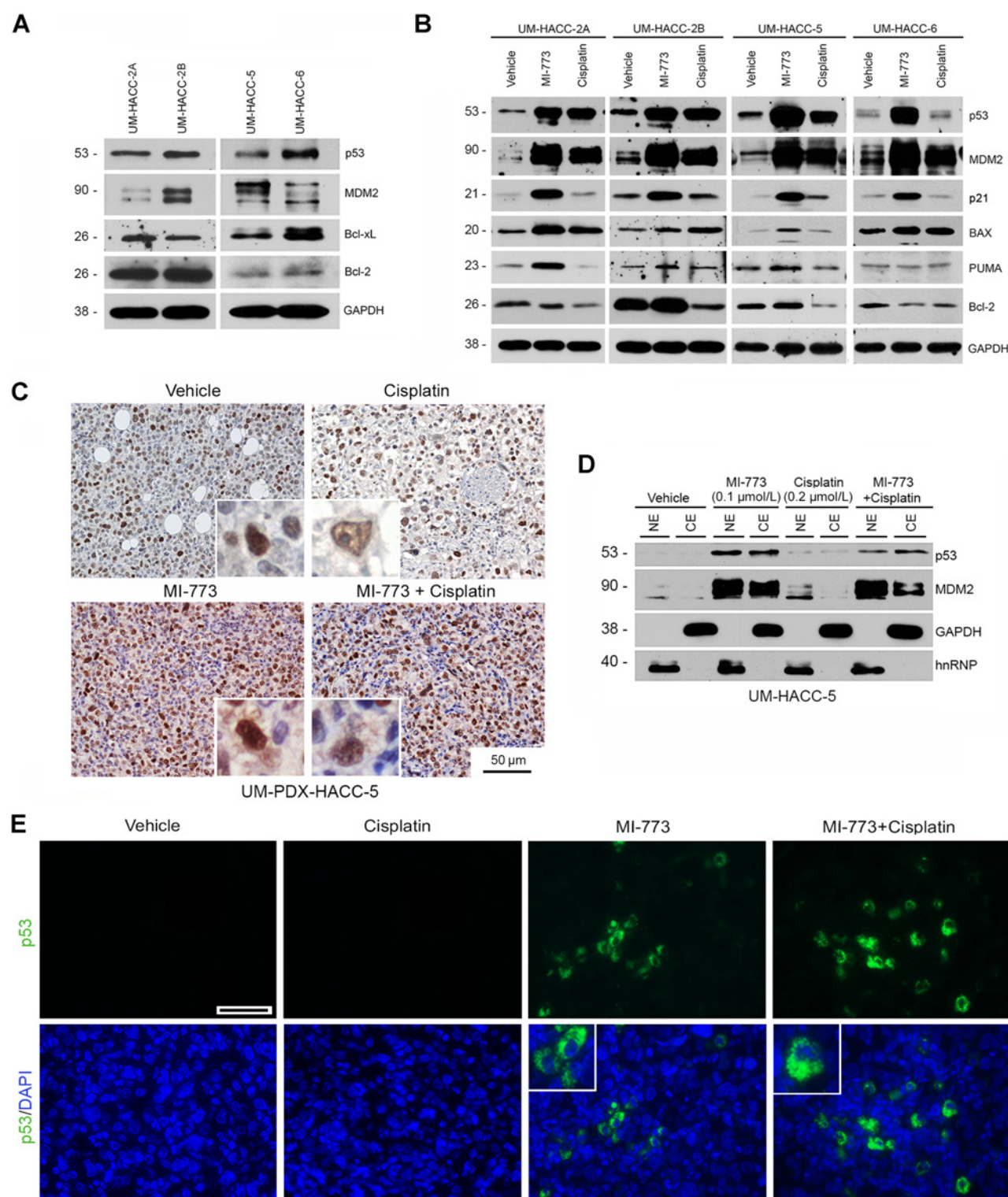
Dosing and frequency of MI-773 determines efficacy

To further explore the antitumor effect of the combined therapy, we designed an independent experiment evaluating weekly versus daily regimens of MI-773 combined with fixed doses of cisplatin. When UM-HACC-PDX-5 tumors reached the average volume of 200 mm³, mice were randomly divided into 5 groups ($n = 7$–8), and treatment was administered for 14 days (Fig. 5). A shorter treatment period was chosen here to focus the evaluation on the posttreatment period. Here, we observed that single drugs, MI-773 or cisplatin, stabilize tumor volume during treatment, but ACC tumor growth resumed as soon as treatment was
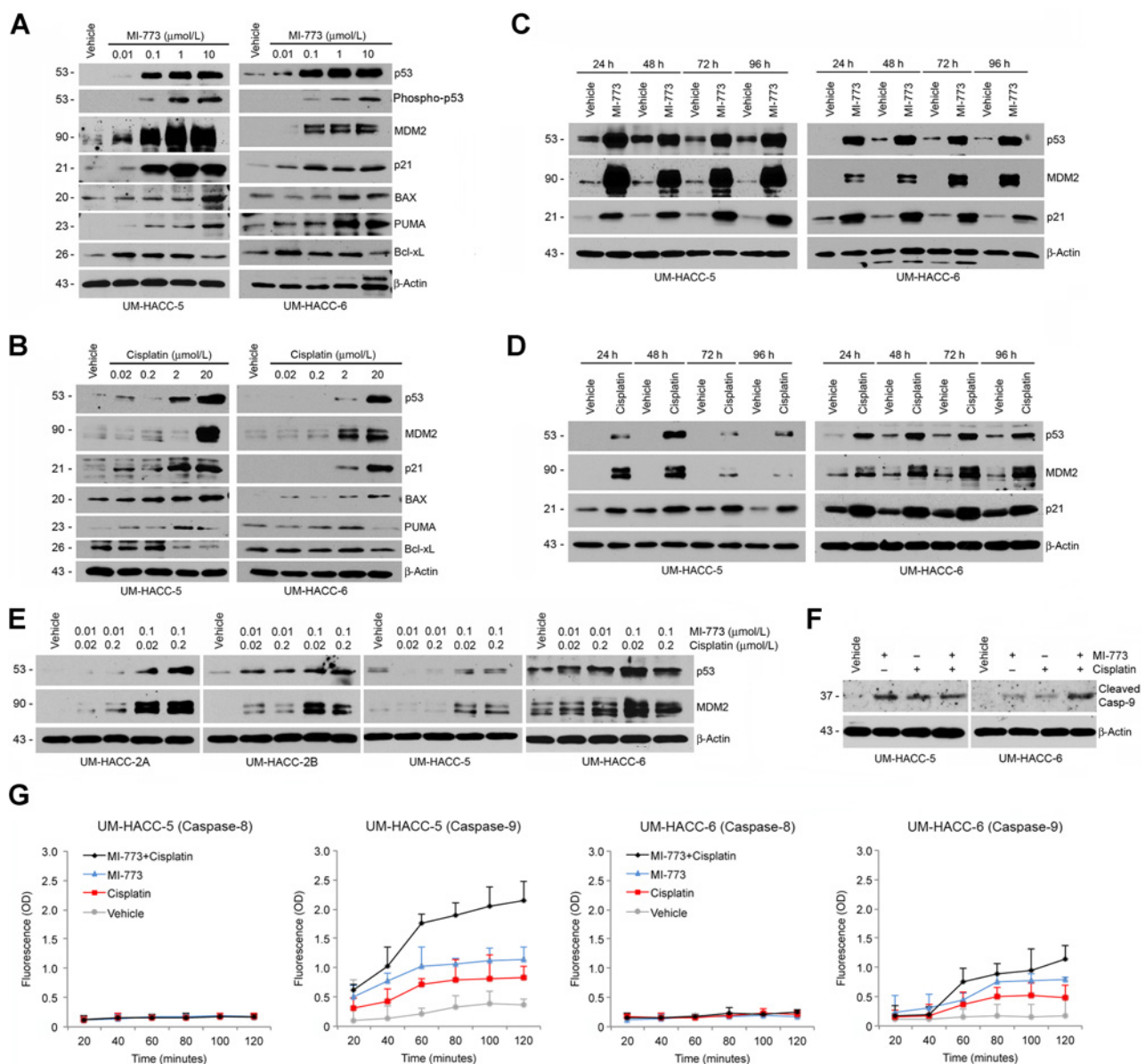
Figure 2.
Effect of MI-773 and/or cisplatin on proliferation and survival of ACC cells. **A,** Graphs depicting time- and dose-dependent assays for the effect of MI-773 and/or cisplatin on the viability of UM-HACC-5 and -6 cells, as determined by SBR assay. Data were normalized against vehicle control and represent at least three independent experiments, done in quadruplicate wells per condition. **B,** Representative photomicrographs of UM-PDX-HACC-5 tumor histologic sections stained for TUNEL (apoptotic cells, green) and DAPI (nuclei, blue) from mice treated either with vehicle control, MI-773, and/or cisplatin (400×). **C,** Graph depicting the percentage of TUNEL-positive cells in 10 random fields per tumor ($n = 4$/group). Different lowercase letters (a, b, and c) indicate statistical difference ($P < 0.05$). **D,** Graphs depicting the effect of the drugs on cell cycle. UM-HACC-5 and -6 cells were exposed to MI-773 and/or cisplatin for 24 hours. The percentage of cells in each cell-cycle phase was determined by propidium iodide staining followed by flow cytometry.

Nör et al.

Figure 3.
Treatment with MI-773 causes changes in p53 status. **A,** Western blot analysis showing basal levels of proteins p53, MDM2, Bcl-x$_L$, and Bcl-2 in UM-HACC-2A, -2B, -5, and -6 cells. **B,** Western blots for p53, MDM2, p21, PUMA, BAX, and Bcl-2 protein expression in UM-HACC cells exposed to predetermined IC$_{50}$ values of MI-773, cisplatin, or vehicle control for 72 hours. **C,** Representative photomicrographs of UM-PDX-HACC-5 histologic sections stained for p53 (brown) and counterstained with hematoxylin (200×). Nuclear p53 is observed in mice treated with vehicle control or cisplatin, while both nuclear (NE) and cytoplasmic (CE) expression of p53 is evidenced in animals exposed to MI-773 as a single agent or combined with cisplatin (details). **D,** Western blot analysis for p53 and MDM2 expression in UM-HACC-5 cells exposed to MI-773 (0.1 µmol/L) and/or cisplatin (0.2 µmol/L) and submitted to a subcellular fractionation assay, to evaluate the nucleus and cytoplasm compartments in separate. **E,** Representative photomicrographs obtained by immunofluorescence for p53 (green), which is located in the cytoplasm (detail) of UM-PDX-HACC-5 cells treated with MI-773 as single drug or combined with cisplatin (400×). Scale bar, 50 µm.
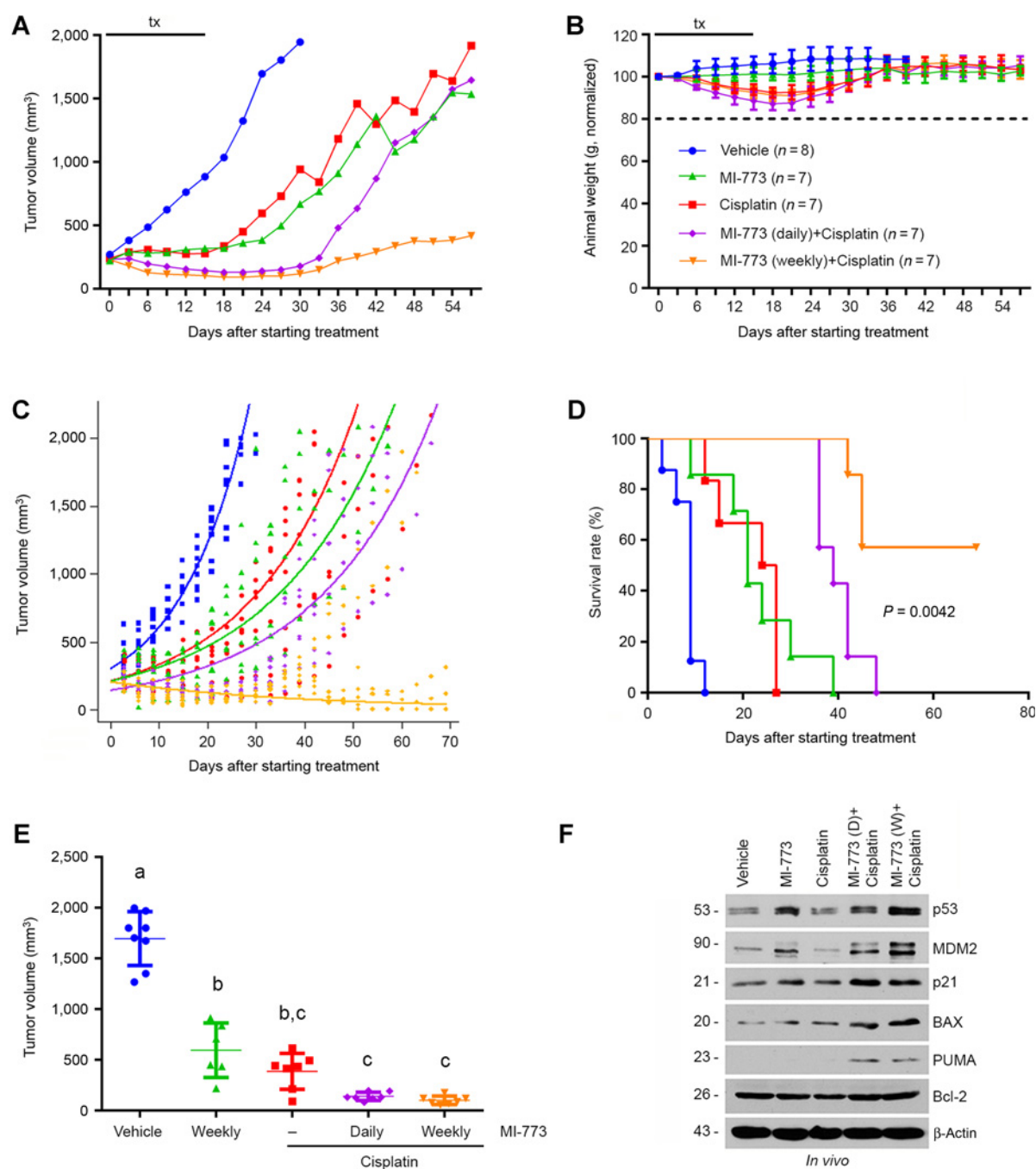
Figure 4.
MI-773 induces apoptosis through PUMA/BAX activation. **A** and **B,** Western blots for phosphorylated and total p53, MDM2, p21, BAX, PUMA, and Bcl-x$_L$ in UM-HACC cells exposed to increasing concentrations of MI-773 (0.01–10 µmol/L) or cisplatin (0.02–20 µmol/L), respectively. **C** and **D,** Western blots for p53, MDM2, and p21 in UM-HACC cells treated with fixed doses of MI-773 (1 µmol/L) or cisplatin (2 µmol/L) for 24 to 96 hours, respectively. **E,** Western blots for p53 and MDM2 in UM-HACC cells upon treatment with lower doses of MI-773 (0.01–0.1 µmol/L) and cisplatin (0.02–0.2 µmol/L) for 24 hours. **F,** Western blots for cleaved caspase-9 in UM-HACC-5 and -6 cells exposed to MI-773 and/or cisplatin for 24 hours. **G,** Graphs depicting activity of caspase-8 or caspase-9 in UM-HACC-5 and -6 cells after 24 hours of treatment with MI-773 and/or cisplatin, as determined by fluorometric assays. OD, optical density. Caspase activity was measured every 20 minutes for a period of 2 hours.

discontinued (Fig. 5A). When MI-773 and cisplatin were combined, daily and weekly MI-773 regimens caused tumor regression. Remarkably, weekly MI-773 combined with cisplatin had a much more prolonged antitumor effect than daily MI-773 combined with cisplatin, even though the total amount of MI-773 administered in both groups was exactly the same (Fig. 5A). Importantly, none of the treatment regimens resulted in mouse weight loss beyond the 20% cutoff (Fig. 5B). We again performed

a linear mixed effect model to evaluate the tumor growth rate over time, now including each dosing strategy as a different factor level. We performed multivariate regression to determine the differences in growth rates between the different treatment approaches. In a model including initial tumor size, overall growth rate, and cisplatin treatment, treatment with MI-773 weekly ($P < 0.0001$), but not daily ($P = 0.6365$), decreased the tumor growth rate (Fig. 5C). In addition, we generated Kaplan–Meier curves using as

Nör et al.

Figure 5.
Effect of MI-773 dosing on long-term efficacy. UM-PDX-HACC-5 tumors were transplanted in immunodeficient mice. When tumors reached 200 mm^3, animals were randomly allocated into five different treatment regimens as follows: 5 mg/kg saline (vehicle control), 200 mg/kg MI-773 (weekly), 5 mg/kg cisplatin, weekly doses of MI-773 (200 mg/kg) combined with 5 mg/kg cisplatin, or daily doses of MI-773 (28.5 mg/kg) combined with 5 mg/kg cisplatin. **A,** Graph depicting tumor volume during treatment (tx) and follow-up (43 days) periods. Weekly regimens of MI-773 combined with cisplatin reduced tumors in size and prevented tumor regrowth compared with the other experimental groups or vehicle control. **B,** Graph depicting mouse weight during the experimental period. Data were normalized against pretreatment weight. **C,** Graph depicting a linear regression model using repeated measures for each tumor over time. Weekly regimens of MI-773 combined with cisplatin significantly decrease the tumor growth rate when compared with daily regimens of MI-773 + cisplatin or single-drug groups ($P < 0.001$). **D,** Kaplan–Meier analysis was done using a 2-fold increase in the tumor volume as a criterion for failure as compared with pretreatment volume. MI-773, cisplatin, or daily MI-773 combined with cisplatin extended time to failure significantly as compared with vehicle control ($P < 0.05$). Graph is depicting the statistical difference between daily and weekly regimens of MI-773 in combination with cisplatin ($P = 0.0042$). **E,** Graph depicting the volume of each individual xenograft tumor at the 10th posttreatment day. Different lowercase letters (a, b, and c) indicate statistical difference ($P < 0.05$). **F,** Western blot analysis for p53, MDM2, p21, BAX, PUMA, and Bcl-2 in UM-PDX-HACC-5 tumors treated with either MI-773 or cisplatin as single agents, weekly or daily regimens of MI-773 combined with cisplatin, or vehicle control. Tumors were harvested 43 days after the last administration of drugs.

criterion for "event" a 2-fold increase in tumor volume as compared with pretreatment size. MI-773, cisplatin, and daily doses of MI-773 combined with cisplatin extended time to failure significantly as compared with vehicle control ($P < 0.05$). Notably, weekly MI-773 combined with cisplatin significantly extended time to failure when compared with daily MI-773 combined with cisplatin ($P = 0.0042$; Fig. 5D). Scatter plot graph was generated to depict tumor volume after 10 days of treatment (Fig. 5E). After 57 days, tumors were collected and processed for protein analysis. As previously noticed (Fig. 1D), therapeutic inhibition of MDM2 by MI-773, as a single agent or combined with cisplatin, causes upregulation of p53, MDM2, and p21 (Fig. 5F). Both daily and weekly combined treatments cause upregulation of apoptosis-related proteins BAX and PUMA. Taken together, the results suggest that weekly MI-773 combined with cisplatin is the preferable treatment schedule in preclinical models of ACC.

Therapeutic inhibition of the MDM2–p53 interaction reduces the fraction of CSCs and prevents recurrence of PDX ACC tumors

It is known that ALDH activity and CD44 expression can be used to identify CSCs in salivary gland tumors (23–26). To elucidate the impact of MI-773 and/or cisplatin treatment on ACC CSCs, mice harboring UM-HACC-PDX-5 tumors were divided in 4 groups ($n = 5$) and received MI-773 (200 mg/kg) for one week, combined or not with two single doses of cisplatin (at the first and seventh day; Fig. 6A). Two days after completion of treatment, tumors were retrieved and the proportion of CSCs was analyzed by flow cytometry. Notably, MI-773 alone (or in combination with cisplatin) decreased the fraction of CSCs (ALDH^{high}CD44^{high}) when compared with cisplatin alone or vehicle control ($P < 0.05$; Fig. 6B and C). Immunofluorescence for ALDH1 suggested the presence of a larger number of ALDH1-positive cells in the vehicle and cisplatin groups, particularly in close proximity to blood vessels and nerves (Supplementary Fig. S4). These findings suggest the existence of perivascular niches for CSCs in ACC, as it has been described for other tumors (29, 30).

It has been postulated that CSCs play an important role in tumor progression, particularly toward locoregional recurrence and/or metastases (31–33). In an attempt to mimic a clinical trial, we treated mice harboring UM-HACC-PDX-5 tumors ($n = 8$) with a neoadjuvant regimen of MI-773, followed by complete surgical resection of the tumor (Fig. 6D). Confirming data described above, a single dose of 200 mg/kg MI-773 significantly decreases the proportion of CSCs (Fig. 6E). Upon follow-up for 300 days (approximately half of the lifetime of a mouse), we observed that 5 (out of 8) mice from the control group presented tumor recurrence (Fig. 6F). Remarkably, not a single mouse from the MI-773–treated group presented tumor recurrence during this experimental period (Fig. 6F and G).

Discussion

ACCs are resistant to all conventional chemotherapeutic drugs available today. As a consequence, treatment for patients with this cancer is largely limited to surgery and radiation. The development of a safe and effective therapy is therefore urgently needed. It is known that MDM2 is overexpressed in ACCs (17, 18). We have recently demonstrated that therapeutic inhibition of the MDM2–p53 interaction with MI-773 mediates short-term antitumor effect in preclinical models of ACC (21). Here, for the first time, we show
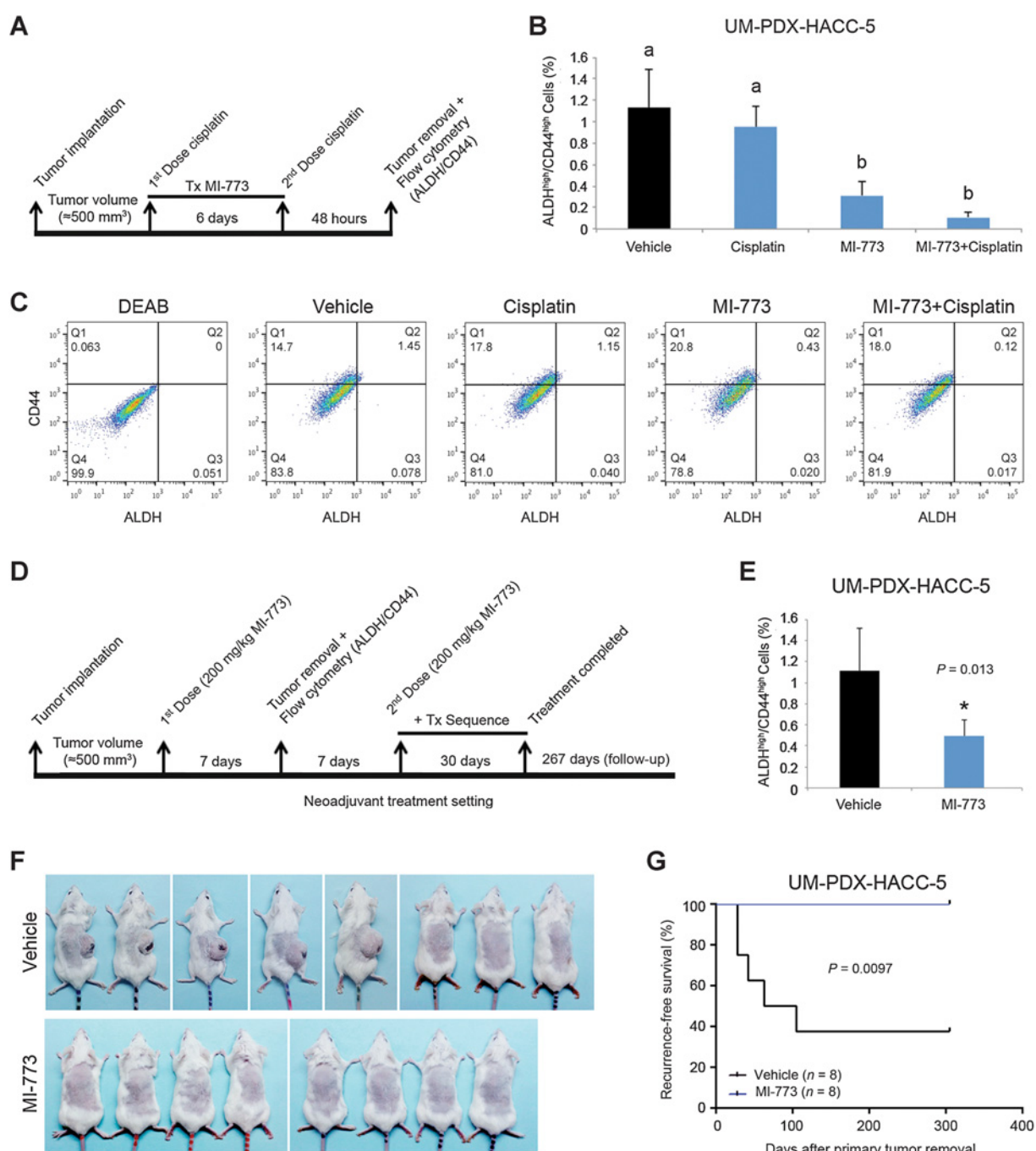
that MI-773 reduces the fraction of ACC cancer stem cells, sensitizes ACC PDXs to cisplatin, and prevents tumor recurrence when used in a neoadjuvant setting.

Mechanisms associated with cancer progression often involve inactivation in p53 tumor suppressor functions, and MDM2 is a common mechanism to inhibit p53 activity (13–16). We demonstrated here that the reactivation of p53 by MI-773 causes a cell-cycle arrest and induces apoptosis of ACC cells. Interestingly, we observed here a partial translocation of p53 from the nucleus to the cytoplasm. Green and Kroemer (34) discussed the cytoplasmic functions of p53 in mitochondrial outer membrane permeabilization–mediated apoptosis. They propose that PUMA (p53-upregulated modulator of apoptosis), a target of nuclear p53, disrupts the Bcl-x$_L$–p53 interaction in the cytoplasm. Thus, p53 is released and forms a complex with BAX, initiating the caspase-dependent apoptotic pathway. Here, we observed the upregulation of BAX in ACC xenograft tumors treated with MI-773 as a single agent or combined to cisplatin. Cisplatin, in turn, was capable of Bcl-2 downregulation in UM-HACC-5 cells. The complementary mechanisms of action of MI-773 and cisplatin might explain the potentiation of the antitumor effect that was observed here when both drugs are used together *in vivo*.

It has been shown that the combination of MI-319 (an alternate small-molecule inhibitor of MDM2 from the class as MI-773) with cisplatin suppressed cell growth, colony formation, and induced apoptosis of pancreatic cancer cells (35). Another study showed that combination of cisplatin with Nutlin-3a, a different class of MDM2 inhibitor, enhanced apoptosis and reverted cisplatin resistance in ovarian cancer cells (36). Interestingly, the inhibition of MDM2–p53 interaction was able to radiosensitize tumor cells in a wide range of cancers types (e.g., lung, breast, colorectal, melanoma, and sarcoma; ref. 37). Our work demonstrated the therapeutic benefit of MI-773 and cisplatin combination in ACCs and offered a new hypothesis to explain the antitumor effect of this drug combination, that is, the ablation of CSCs. In addition, we demonstrated here that MI-773 decreases the risk of locoregional recurrence in preclinical models, which is likely associated with its effect on eliminating at least in part the highly tumorigenic CSCs.

The long-term prognosis of patients with ACC is directly affected by late episodes of recurrence and/or metastases (10). In head and neck squamous cell carcinomas, resistance to chemotherapy and recurrence has been associated with CSCs (22, 29, 38). This small population of uniquely tumorigenic cells was also found in salivary gland tumors (25, 26), but their sensitivity to chemotherapy is not understood. Here, we observed that cisplatin did not have a significant effect on the fraction of CSCs in ACC xenograft tumors. In contrast, MI-773 significantly reduced the fraction of CSCs when compared with cisplatin or vehicle control. This finding raises a putative hypothesis to explain the long-term antitumor effect of this drug combination *in vivo*, that is, MI-773 targets the CSCs (resistant to cisplatin) that have been shown to be mediators of tumor recurrence and/or metastases (33, 33). Indeed, when we exposed mice to a neoadjuvant treatment of MI-773 (i.e., a single dose of MI-773 followed by surgical removal of the tumor, and a subsequent MI-773 therapy for 30 days), we confirmed the reduction of CSCs in the excised tumors. Notably, no recurrence was observed in mice treated with MI-773 even after 300 days of follow-up (about half of the lifetime of mice), while more than half of the mice that received vehicle presented recurrent tumors.

Nör et al.

Figure 6.
MI-773 reduces the fraction of CSCs and prevents recurrence in ACC xenograft tumors. **A,** Timeline showing the experimental design. **B,** Graph depicting the fraction of CSCs (ALDH^{high}CD44^{high}) identify by flow cytometry in xenograft tumors treated with 5 mg/kg cisplatin and/or 200 mg/kg MI-773. Different lowercase letters (a and b) indicate significant differences among groups ($P < 0.05$). **C,** Graphs depicting the flow cytometry gates for the percentage of CSCs (Q2) in UM-PDX-HACC-5 tumors treated with cisplatin and/or MI-773. DEAB is showing the control of the reaction. **D,** Timeline showing the neoadjuvant treatment (Tx) design. **E,** Graph depicting the fraction of CSCs (ALDH^{high}CD44^{high}) identify by flow cytometry in UM-PDX-HACC-5 tumors treated with MI-773 or vehicle control. **F,** Macroscopic view of mice harboring recurrent tumors or tumor-free animals at the end of the experiment. **G,** Kaplan–Meier curve depicting recurrence-free survival in mice treated either with 200 mg/kg MI-773 or vehicle control. Recurrence was defined as the presence of a palpable tumor.

In conclusion, this work demonstrated that therapeutic inhibition of the MDM2–p53 interaction with MI-773 is an effective antitumor strategy that mediates ACC tumor regression, reduces the fraction of CSCs, sensitizes xenograft tumors to cisplatin, and prevents tumor recurrence in preclinical models of ACC. These preclinical data provide the conceptual framework for an early

phase I trial testing a combination therapy of MI-773 and cisplatin for treatment of patients with recurrent/metastatic ACC. Once clinical efficacy is established, a step further would be the testing of MI-773 as an adjuvant or neoadjuvant therapy along with surgical resection of the tumor.

Disclosure of Potential Conflicts of Interest

S. Wang reports receiving other commercial research support from and holds ownership interest (including patents) in Ascenta Therapeutics. No potential conflicts of interest were disclosed by the other authors.

Authors' Contributions

Conception and design: F. Nör, G.A. Acasigua, J.E. Nör
Development of methodology: F. Nör, K.A. Warner, G.A. Acasigua, J.E. Nör
Acquisition of data (provided animals, acquired and managed patients, provided facilities, etc.): K.A. Warner, G.A. Acasigua, S.A. Kerk, J.I. Helman
Analysis and interpretation of data (e.g., statistical analysis, biostatistics, computational analysis): F. Nör, G.A. Acasigua, A.T. Pearson, M. Sant'Ana Filho, J.E. Nör
Writing, review, and/or revision of the manuscript: F. Nör, K.A. Warner, G.A. Acasigua, A.T. Pearson, S.A. Kerk, J.I. Helman, M. Sant'Ana Filho, J.E. Nör
Administrative, technical, or material support (i.e., reporting or organizing data, constructing databases): Z. Zhang, G.A. Acasigua

Study supervision: Z. Zhang, M. Sant'Ana Filho, J.E. Nör
Other (provided the MDM2–p53 interaction inhibitor): S. Wang

References

1. Coca-Pelaz A, Rodrigo JP, Bradley PJ, Vander Poorten V, Triantafyllou A, Hunt JL, et al. Adenoid cystic carcinoma of the head and neck – An update. Oral Oncol 2015;51:652–61.
2. Kowalski PJ, Paulino AF. Perineural invasion in adenoid cystic carcinoma: its causation/promotion by brain-derived neurotrophic factor. Hum Pathol 2002;33:933–6.
3. Chae YK, Chung SY, Davis AA, Carneiro BA, Chandra S, Kaplan J, et al. Adenoid cystic carcinoma: current therapy and potential therapeutic advances based on genomic profiling. Oncotarget 2015;6:37117–34.
4. Dillon PM, Chakraborty S, Moskaluk CA, Joshi PJ, Thomas CY. Adenoid cystic carcinoma: a review of recent advances, molecular targets, and clinical trials. Head Neck 2014;38:620–7.
5. Dodd RL, Slevin NJ. Salivary gland adenoid cystic carcinoma: a review of chemotherapy and molecular therapies. Oral Oncol 2006;42:759–69.
6. Ghosal N, Mais K, Shenjere P, Julyan P, Hastings D, Ward T, et al. Phase II study of cisplatin and imatinib in advanced salivary adenoid cystic carcinoma. Br J Oral Maxillofac Surg 2011;49:510–5.
7. Andry G, Hamoir M, Locati LD, Licitra L, Langendijk JA. Management of salivary gland tumors. Expert Rev Anticancer Ther 2012;12:1161–8.
8. Licitra L, Cavina R, Grandi C, Palma SD, Guzzo M, Demicheli R, et al. Cisplatin, doxorubicin and cyclophosphamide in advanced salivary grand carcinoma. A phase II trial of 22 patients. Ann Oncol 1996;7:640–2.
9. Ross PJ, Teoh EM, A'hern RP, Rhys-Evans PH, Harrington KJ, Nutting CM, et al. Epirubicin, cisplatin and protracted venous infusion 5-fluorouracil chemotherapy for advanced salivary adenoid cystic carcinoma. Clin Oncol (R Coll Radiol) 2009;21:311–4.
10. Lloyd S, Yu JB, Wilson LD, Decker RH. Determinants and patterns of survival in adenoid cystic carcinoma of head and neck, including an analysis of adjuvant radiation therapy. Am J Clin Oncol 2011;34:76–81.
11. Wong SJ, Karrison T, Hayes DN, Kies MS, Cullen KJ, Tanvetyanon T, et al. Phase II trial of dasatinib for recurrent or metastatic c-KIT expressing adenoid cystic carcinoma and for nonadenoid cystic malignant salivary tumors. Ann Oncol 2016;27:318–23.
12. Ganly I, Amit M, Kou L, Palmer FL, Migliacci J, Katabi N, et al. Nomograms for predicting survival and recurrence in patients with adenoid cystic carcinoma. An international collaborative study. Eur J Cancer 2015;51:2768–76.
13. Hainaut P, Hollstein M. p53 and human cancer: the first ten thousand mutations. Adv Cancer Res 2000;77:81–137.
14. Daujat S, Neel H, Piette J. MDM2: life without p53. Trends Genet 2001;17:459–64.
15. Wu X, Bayle JH, Olson D, Levine AJ. The p53-mdm2 autoregulatory feedback loop. Genes Dev 1993;7:1126–32
16. Momand J, Wu HH, Dasgupta G. MDM2-master regulator of the p53 tumor suppressor protein. Gene 2000;242:15–29.
17. Araújo VC, Martins MT, Leite KR, Gomez RS, Araújo NS. Immunohistochemical MDM2 expression in minor salivary gland tumours and its relationship to p53 gene status. Oral Oncol 2000;36:67–9.
18. de Lima Mde D, Marques YM, Alves Sde MJr, Freitas VM, Soares FA, de Araújo VC, et al. MDM2, P53, P21WAF1 and pAKT protein levels in genesis and behaviour of adenoid cystic carcinoma. Cancer Epidemiol 2009;33:142–6.
19. Wang S, Sun W, Zhao Y, McEachern D, Meaux I, Barrière C, et al. SAR405838: an optimized inhibitor of MDM2-p53 interaction that induces complete and durable tumor regression. Cancer Res 2014;74:5855–65.
20. Zhao Y, Aguilar A, Bernard D, Wang S. Small-molecule inhibitors of the MDM2-p53 protein-protein interaction (MDM2 Inhibitors) in clinical trials for cancer treatment. J Med Chem 2015;58:1038–52.
21. Warner K, Nor F, Acasigua G, Martins M, Zhang Z, McLean SA, et al. Targeting MDM2 for treatment of adenoid cystic carcinoma. Clin Cancer Res 2016 2016;22:3550–9.
22. Nör C, Zhang Z, Warner KA, Bernardi L, Visioli F, Helman JI, et al. Cisplatin induces Bmi-1 and enhances the stem cell fraction in head and neck cancer. Neoplasia 2014;16:137–46.
23. Acasigua GA, Warner KA, Nör F, Helman J, Pearson AT, Fossati AC, et al. BH3-mimetic small molecule inhibits the growth and recurrence of adenoid cystic carcinoma. Oral Oncol 2015;51:839–47.
24. Pearson AT, Finkel KA, Warner KA, Nör F, Tice D, Martins MD, et al. Patient-derived xenograft (PDX) tumors increase growth rate with time. Oncotarget 2016;7:7993–8005.
25. Adams A, Warner K, Nör JE. Salivary gland cancer stem cells. Oral Oncol 2013;49:845–53.
26. Adams A, Warner K, Pearson AT, Zhang Z, Kim HS, Mochizuki D, et al. ALDH/CD44 identifies uniquely tumorigenic cancer stem cells in salivary gland mucoepidermoid carcinomas. Oncotarget 2015;29:26633–50.
27. Zhang Z, Neiva KG, Lingen MW, Ellis LM, Nör JE. VEGF-dependent tumor angiogenesis requires inverse and reciprocal regulation of VEGFR1 and VEGFR2. Cell Death Differ 2010;17:499–512.
28. Wagner JM, Karnitz LM. Cisplatin-induced DNA damage activates replication checkpoint signaling components that differentially affect tumor cell survival. Mol Pharmacol 2009;76:208–214.

Nör et al.

29. Krishnamurthy S, Nör JE. Head and neck cancer stem cells. J Dent Res 2012;91:334–340.
30. Ritchie KE, Nör JE. Perivascular stem cell niche in head and neck cancer. Cancer Lett 2013;338:41–6.
31. Reya T, Morrison SJ, Clarke MF, Weissman IL. Stem cells, cancer, and cancer stem cells. Nature 2001;414:105–11.
32. Chinn SB, Darr OA, Owen JH, Bellile E, McHugh JB, Spector ME, et al. Cancer stem cells: mediators of tumorigenesis and metastasis in head and neck squamous cell carcinoma. Head Neck 2015;37:317–26.
33. Islam F, Gopalan V, Smith RA, Lam AK. Translational potential of cancer stem cells: a review of the detection of cancer stem cells and their roles in cancer recurrence and cancer treatment. Exp Cell Res 2015;335:135–47
34. Green DR, Kroemer G. Cytoplasmic functions of the tumour suppressor p53. Nature 2009;458:1127–30.
35. Azmi AS, Aboukameel A, Banerjee S, Wang Z, Mohammad M, Wu J, et al. MDM2 inhibitor MI-319 in combination with cisplatin is an effective treatment for pancreatic cancer independent of p53 function. Eur J Cancer 2010;46:1122–31.
36. Mir R, Tortosa A, Martinez-Soler F, Vidal A, Condom E, Pérez-Perarnau A, et al. MDM2 antagonists induce apoptosis and synergize with Cisplatin overcoming chemoresistance in TP53 wild-type ovarian cancer cells. Int J Cancer 2013;132:1525–36.
37. Werner LR, Huang S, Francis DM, Armstrong EA, Ma F, Li C, et al. Small molecule inhibition of MDM2-p53 interaction augments radiation response in human tumors. Mol Cancer Ther 2015;14:1994–2003.
38. Zhang Z, Filho MS, Nör JE. The biology of head and neck cancer stem cells. Oral Oncol 2012;48:1–9.

Clinical Cancer Research

Therapeutic Inhibition of the MDM2−p53 Interaction Prevents Recurrence of Adenoid Cystic Carcinomas

Felipe Nör, Kristy A. Warner, Zhaocheng Zhang, et al.

Updated version	Access the most recent version of this article at: doi:10.1158/1078-0432.CCR-16-1235
Supplementary Material	Access the most recent supplemental material at: http://clincancerres.aacrjournals.org/content/suppl/2016/08/20/1078-0432.CCR-16-1235.DC1

Cited articles	This article cites 38 articles, 7 of which you can access for free at: http://clincancerres.aacrjournals.org/content/23/4/1036.full.html#ref-list-1

E-mail alerts	Sign up to receive free email-alerts related to this article or journal.
Reprints and Subscriptions	To order reprints of this article or to subscribe to the journal, contact the AACR Publications Department at pubs@aacr.org.
Permissions	To request permission to re-use all or part of this article, contact the AACR Publications Department at permissions@aacr.org.